Hindawi
International Journal of Antennas and Propagation
Volume 2020, Article ID 1238656, 8 pages
https://doi.org/10.1155/2020/1238656

*Research Article*

# Design of Wideband Absorber Based on Dual-Resistor-Loaded Metallic Strips

**Mingxi Zhang,[1,2] Binchao Zhang,[3] Xiaochun Liu,[2] Shining Sun,[2] and Cheng Jin[3]**

[1]*College of Electronic and Information Engineering, Nanjing University of Aeronautics and Astronautics, Nanjing, Jiangsu, China*
[2]*Aviation Key Laboratory of Science and Technology on High Performance Electromagnetic Windows, Ji'nan, Shandong, China*
[3]*School of Information and Electronics, Beijing Institute of Technology, Beijing 100081, China*

Correspondence should be addressed to Binchao Zhang; zhangbinchao@bit.edu.cn

Received 28 February 2020; Revised 17 April 2020; Accepted 6 May 2020; Published 18 May 2020

Academic Editor: Renato Cicchetti



A method for designing a dual-polarized wideband absorber with low profile by using dual-resistor-loaded metallic strips is proposed in this paper. Each unit cell consists of a resistive sheet with dual-resistor-loaded metallic strips and an underlying conducting plate. Two-dimensional arrays of two unequal metallic strips are printed on the dielectric substrate, and two resistors are embedded in the metallic strips. By properly designing the resonant frequencies of these metallic strips, a wide absorption band with three resonances is obtained. An equivalent circuit model is introduced, and the current distributions are examined to understand the physical mechanism of the proposed absorber. An example of the absorber is fabricated and measured to verify our designed concept. The measured results show that the wideband absorption performance with a fractional bandwidth of 129% under the normal incidence and the stable angular response are achieved. In addition, the proposed absorber has a low profile with $0.08\lambda_L$, where $\lambda_L$ is the wavelength at the lowest operating frequency.

## 1. Introduction

Electromagnetic (EM) absorbers have been an intriguing area for their miscellaneous applications, such as improving electromagnetic compatibility of the integrated circuits, eliminating electromagnetic interferences in complicated environments, and being adapted as the chipless radio-frequency indemnification tags [1–3]. Most applications of EM absorbers require wide bandwidth and low profile with more than 10 dB reflection reduction, which limits the extensive usage of classic absorbers, such as Salisbury screens [4] or multilayer Jaumann absorbers [5]. The theoretical minimum thickness for a given absorption performance was depicted in [6], which motivated the development of the frequency selective surface (FSS) pattern used in the lossy layer of the absorber [7].

The circuit analog (CA) absorber with a lossy FSS printed on a low-loss substrate backed by a perfect conducting plane is an attractive candidate to approximate the Rozanov limit. In the past, the perception of multiple resonances was employed to widen the absorption bandwidth [8–11]. For the single-layer CA absorber, the design in [12] has achieved a wide absorption bandwidth with three resonances. Similarly, two-layer configuration and loop arrays embedded with chip resistors were utilized to build a wide absorption band [13, 14]. An alternative design, replacing the RLC resonating circuits with low-pass RC circuits, was proposed to design wideband absorbers utilizing multilayer structures with the overall thickness approximating the Rozanov limit [15, 16].

Except the aforementioned planar absorber, a new structure named three-dimensional (3D) absorber is another effective approach to obtain wide absorption band [17]. The cavity along the $z$-direction is utilized to establish the absorption band, and the energy is absorbed by the multiple resonant modes in the air and substrate regions [18]. However, it usually needs a relatively thick profile to accommodate the multiresonant structure, and it also has a complex configuration. In addition, active absorbers provide potentials to break the Rozanov limit [19]. Negative

inductors were used for actively matching the equivalent inductance of the thin conductor-backed spacer, and the bandwidth ratio could be larger than 6 : 1 with the thickness of only $0.015\lambda_L$, where $\lambda_L$ is the wavelength at the lowest operating frequency. Unfortunately, the negative inductors are nonnatural devices, and they are difficult to be realized.

In this paper, the design of dual-polarized and wideband absorber with two unequal dual-resistor-loaded metallic strips is presented. The lossy layer of the unit cell consists of two orthogonal strips printed on both sides of a dielectric substrate, and two-dimensional arrays of two unequal resistor-loaded metallic strips are printed on each side of the dielectric substrate. By properly designing the resonant frequencies of these two metallic strips, a wide absorption band with three resonances is obtained. An equivalent circuit model is introduced, and the current distributions along the strips are examined to demonstrate the physical mechanism of the proposed absorber with three resonant frequencies. In order to verify our design concept, an example is designed and fabricated, which shows a wideband absorption performance for dual polarizations and stable angular response.

## 2. Design and Analysis

*2.1. Configuration of the Unit Cell.* As a component of the CA absorber, the lossy layer plays an important role in impedance matching at the interface between the absorber and the air space, and it needs to be carefully designed for wideband performance. Then, the incident EM wave will be absorbed by the resistive component in the lossy layer. In our proposed structure, the lossy layer is implemented by the resistor-loaded frequency selective surface, and its geometry is illustrated in Figure 1. In each unit cell, the lossy layer consists of two orthogonal components printed on both sides of a dielectric substrate with a relative dielectric constant $\varepsilon_r$ of 4.4, loss tangent $\tan\delta$ of 0.02, and thickness $t$ of 0.5 mm to realize a dual-polarized absorber, as shown in Figures 1(a) and 1(b). On each side, there are two shorter dual-resistor-loaded metallic strips with the length $l_2$ of 9.5 mm symmetrically located on either side of a dual-resistor-loaded metallic strip with the length $l_1$ of 27 mm arranged diagonally, and the distance $d$ between these two types of metallic strips is 8 mm. In addition, the width $w$ of the metallic strip is 0.5 mm, the period $p$ of the unit cell is 20 mm, and the thickness $h$ of the air spacer is 8 mm. Moreover, a conducting plate is placed under the lossy layer to keep a good absorption performance.

*2.2. Operating Principle.* In order to intuitively understand the absorption mechanism, the equivalent circuit model of the proposed absorber is given, as shown in Figure 2. It is found that the lossy layer is equivalent to a pair of parallel *RLC* circuits, and it is connected with the ground across a transmission line circuit. Two resistor-loaded metallic strips will result in two series *RLC* circuits in parallel [20]. In the circuit, $R_1$, $L_1$, and $C_1$ represent the equivalent resistance, inductance, and capacitance of the longer metallic strip, respectively, while $R_2$, $L_2$, and $C_2$ denote those of shorter metallic strips. In addition, the short-circuited transmission line with electric length $\theta$ represents the grounded air spacer.

Then, the input admittance $Y_{\text{in}}$ of the proposed absorber can be expressed as

$$Y_{\text{in}} = \sum_{i=1}^{2} \frac{1}{R_i + j\left(\omega L_i - \left(1/\omega C_i\right)\right)} - jY_0 \cot\beta h, \tag{1}$$

where $\beta = 2\pi/\lambda$ is the wavenumber and $Y_0$ is the characteristic admittance of the free space. The initial values of $L_1$, $C_1$, $L_2$, and $C_2$ under normal incidence can be obtained from their geometric relationship, which has been studied in detail [21]:

$$\frac{X_L}{Z_0} = \frac{l}{\lambda}\left[\ln\left(\csc\frac{\pi w}{2p}\right) + G(p, w, \lambda)\right], \tag{2}$$

where $Z_0$ is the characteristic impedance of the free space, $l$ and $w$ are the length and width of the metallic strip, respectively, and $G(p, w, \lambda)$ is the correction term available, which is studied minutely in [22, 23].

Therefore, the reflection coefficient of the proposed absorber can be calculated as

$$\Gamma = \frac{Z_{\text{in}} - Z_0}{Z_{\text{in}} + Z_0} = \frac{\left(Z_{\text{in}}^{\text{Re}} - Z_0\right) + jZ_{\text{in}}^{\text{Im}}}{\left(Z_{\text{in}}^{\text{Re}} + Z_0\right) + jZ_{\text{in}}^{\text{Im}}}, \tag{3}$$

where $Z_{\text{in}} = 1/Y_{\text{in}}$ is the input impedance and $Z_{\text{in}}^{\text{Re}}$ and $Z_{\text{in}}^{\text{Im}}$ are the real and the imaginary part of the input impedance. In order to realize a good absorption performance in a wide frequency band, the reflection coefficient needs to approach zero in the operating frequency band, which can be satisfied when

$$\Gamma = 0 \longrightarrow \begin{cases} Z_{\text{in}}^{\text{Re}} = Z_0, \\ Z_{\text{in}}^{\text{Im}} = 0. \end{cases} \tag{4}$$

The simulated input impedance of the proposed absorber is shown in Figure 3. The real part of input impedance oscillates around 377 Ω, and three peaks appear at $f_1$, $f_2$, and $f_3$. In addition, the imaginary part oscillates around zero; thus, the reflection coefficient equals to zero in the operating frequency band according to (4). Then, the incident wave will illuminate the absorber with no reflection and be absorbed by the resistive components finally.

Figure 4 compares the absorption performances of the equivalent circuit model and ANSYS HFSS simulation under the normal incidence, which exhibits a good agreement. Additionally, the cross-polarized reflection coefficient of the absorber is also shown to indicate a negligible cross-polarization response. The dimensions of the proposed absorber are carefully designed to achieve a good absorption performance. The initial values of lumped inductances and capacitances utilized in the equivalent circuit model are obtained using the formulas presented in [21–23] as the following values: $L_1 = 19.1$ nH, $C_1 = 0.017$ pF, $L_2 = 7.17$ nH, and $C_2 = 0.081$ pF.

The simulated result shows that a wide absorption band is obtained from 3.08 to 14.02 GHz, and the absorptivity is greater than 90% in the absorption band. It should be

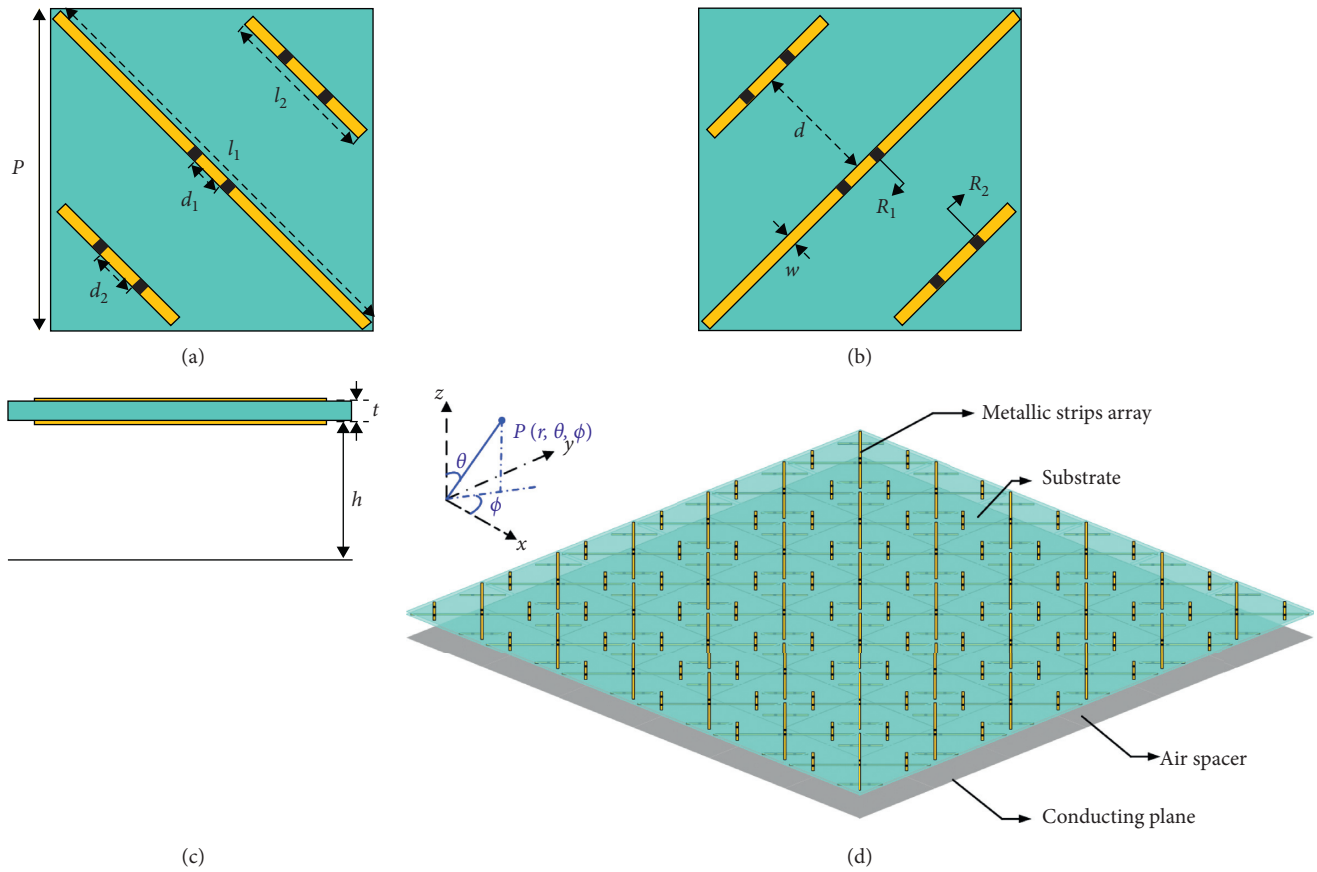


FIGURE 1: Configuration of the designed absorber. (a) Top surface of the substrate. (b) Bottom surface of the substrate. (c) Side view. (d) 3D view. $p = 20$, $h = 7.5$, $l_1 = 27$, $l_2 = 9.5$, $d_1 = 1.5$, $d_2 = 2.5$, $d = 8$, $w = 0.5$, and $t = 0.5$ (all dimensions are in mm).

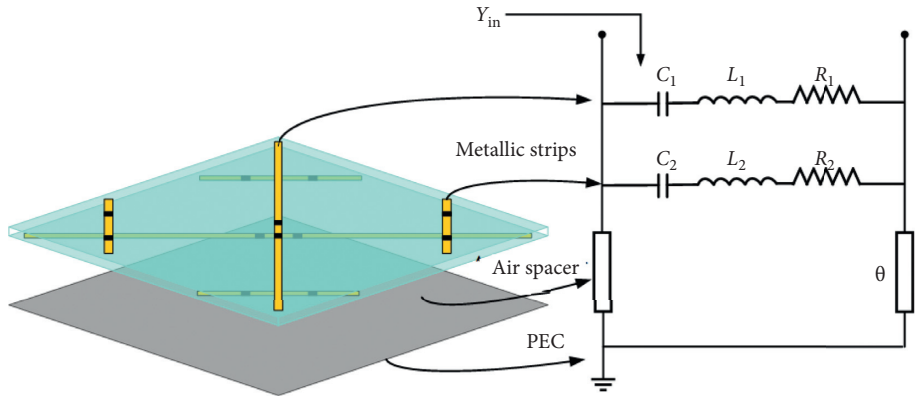


FIGURE 2: Equivalent circuit model of the proposed absorber for normal incidence with TE polarization.

mentioned that the absorptivity is calculated as $1 - |\Gamma|^2$ because of the existence of the conducting plane. Furthermore, there are three reflection zeros in the absorption band, namely, $f_1 = 3.64$ GHz, $f_2 = 8.32$ GHz, and $f_3 = 12.96$ GHz.

The simulated current distributions of the proposed absorber at three reflection zeros are shown in Figure 5 to gain physical insight into the existence of three resonances. Without loss of generality, we assume that the incident field is TE-polarized, and its amplitude is 1 V/m. It is found that the resonance at $f_1$ is mainly caused by the fundamental resonant mode of the central longer metallic strip, as shown in Figure 5(a). We can observe that a wave antinode is generated in the center, and the current will pass through the embedded resistors and be consumed finally. The resonant frequency can be calculated by

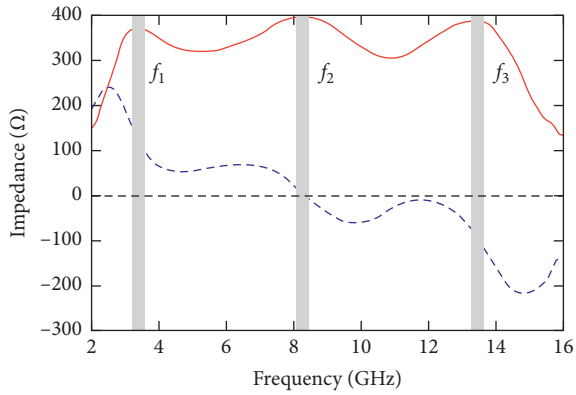


Figure 3: Input impedance of the proposed absorber.

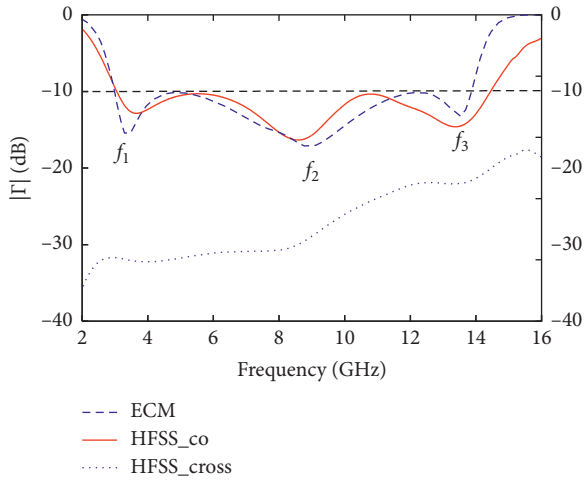


Figure 4: Simulated and calculated reflection coefficients of the proposed absorber.

$$f = \frac{c}{2l * \sqrt{\varepsilon_{r,\text{eff}}}}, \tag{5}$$

where $l$ is the length of the metallic strip, $c$ is the velocity of light, and $\varepsilon_{r,\text{eff}}$ is the effective relative permittivity, which was calculated in [13].

In addition, Figures 5(b) and 5(c) depict the current distributions at $f_2$ and $f_3$, which are corresponding to the first odd resonant mode with two wave antinodes of the central longer metallic strip and the fundamental mode with one wave antinode of the shorter metallic strip, respectively. We can also observe that slight currents are excited on two shorter metallic strips at the resonant frequency $f_2$, and the same situation happens at the resonant frequency $f_3$, which is caused by the coupling between two metallic strips at these two resonant frequencies.

It is well known that the first odd resonance cannot be excited under normal incidence [7] because the symmetric current with opposite directions generated in a receiving dipole-like metallic strip counteracts each other at the resonant frequency. However, our proposed structure can be considered as a superposition of two asymmetrical-dipole-like metallic strips, and two chip resistors are inserted at different feeding ports. The current excited at the first odd resonance is asymmetrical, as shown in Figure 5(b), resulting in a nonzero current [11]. Then, two resistors are loaded on the metallic strip in our proposed structure to realize the excitement of the first odd resonance.

*2.3. Parameter Discussion.* According to the analysis of the operating principle in Section 2.2, four parameters are studied here to reveal their effect on the resonant characteristic of the proposed absorber, which are the lengths $l_1$ and $l_2$ of the metallic strips and the resistive values $R_1$ and $R_2$ of the embedded chip resistors.

The values of loaded dual-chip-resistors should be optimized carefully to achieve a superior absorption performance. Figure 6 shows different frequency responses with various values of the chip resistor. There are two degrees of freedom that one of the two chip resistors is tuned when another is fixed. Figure 6(a) exhibits that the value of $R_1$ influences the frequency response of the longer metallic strip, and the absorption performance is good when $R_1$ is set to 120 Ω. On the contrary, the value of $R_2$ can impact the frequency response of shorter metallic strips, as shown in Figure 6(b), and it is chosen to 70 Ω to get a wider absorption band and good absorption performance.

Figure 7 indicates the variation of the reflection zeros with different values of the length $l_1$ of the longer strip and $l_2$ of the shorter strip. The reflection zero of $f_1$ and $f_2$ shifts to a lower frequency and $f_3$ almost unchanged when $l_1$ increases, as shown in Figure 7(a). Because $f_1$ and $f_2$ are the fundamental and the first odd resonant mode of the longer strip, increasing $l_1$ will enlarge the resonant wavelength. Figure 7(b) illustrates the influence on three reflection zeros when $l_2$ increases; it is found that $f_2$ and $f_3$ move to a lower frequency while $f_1$ is fixed. Increasing $l_2$ will result in a large resonant wavelength of the shorter strip, and it will also increase the resonant wavelength of the longer strip because of the coupling between these two strips.

Then, a wideband absorption performance can be obtained with properly designed aforementioned parameters, as shown in Figure 4. For the certain performance of absorption, including the bandwidth and absorptivity, there is a physical boundary for the thickness of the nonmagnetic absorber, defined as Rozanov limit [6]:

$$\text{RL} \geq \frac{\left|\int_0^\infty \ln|\Gamma(\lambda)|\,d\lambda\right|}{2\pi^2}, \tag{6}$$

where RL is the Rozanov limit and $\Gamma(\lambda)$ is the reflection coefficient of the wavelength response. In this paper, our designed absorber has the Rozanov limit of 7.36 mm calculated by (6). Compared with the realized thickness of the absorber, there is only 8% thicker than the Rozanov limit.

## 3. Measurement Verification

A prototype is fabricated with an array of $15 \times 15$ unit cells to verify the absorption performance of the designed

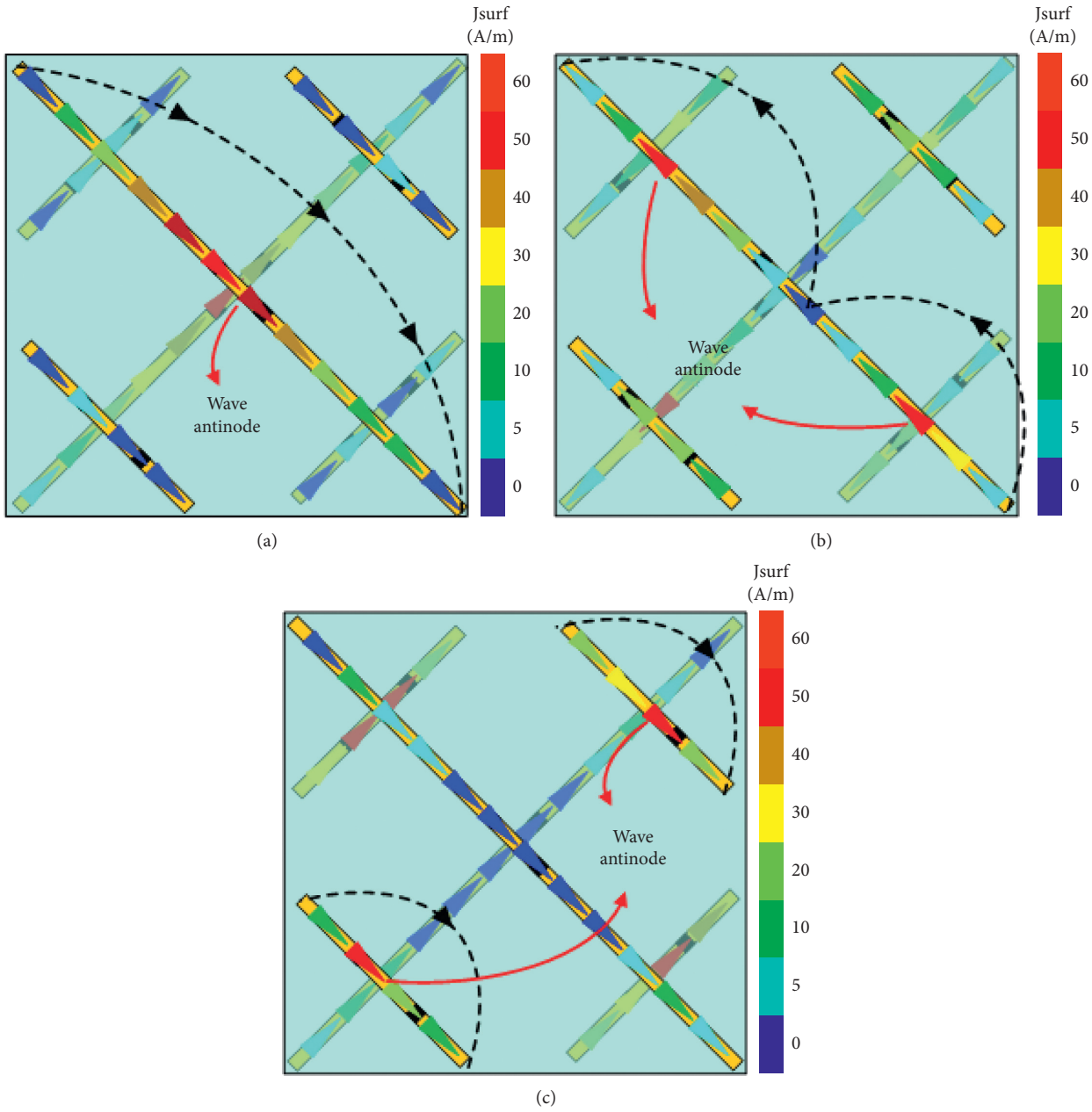


Figure 5: Simulated current distributions of the proposed absorber at three resonant frequencies of (a) $f_1 = 3.64$ GHz, (b) $f_2 = 8.32$ GHz, and (c) $f_3 = 12.96$ GHz.

absorber, and the total size of the prototype is 300 mm × 300 mm. Both chip resistors and metallic strips are printed on the FR4 substrate, and the plastic screws are used to separate the lossy layer and metallic ground with a certain distance of 7.5 mm, as shown in Figure 8(b). Additionally, the commercial product of the chip resistors we used in the realized absorber prototype is RF0402-120R-HS and RF0402-69R8-HS. The prototype is measured in an anechoic chamber, which has an arched frame mounted with two horn antennas, as shown in Figure 8(a). Then, the measured reflection coefficients for normal and oblique incident waves are obtained by adjusting the angle position of two horn antennas.

The measured results show that our designed absorber has a wideband absorption performance and stable angular response, as shown in Figure 9. It is found that the absorption band is from 3.1 to 14.2 GHz with a fractional bandwidth of 129% under the normal incidence. In addition, the absorption performances of the designed absorber are relatively stable when the incidence angle increases up to 30° for both TE and TM polarizations, as shown in Figure 9. It is seen that the resonant frequencies of $f_3$ shift to a lower frequency, and the width of the absorption band becomes narrower when the incident angle increases, which is caused by the nonnegligible parasitic capacitance and inductance of the used chip resistors in the high frequency.

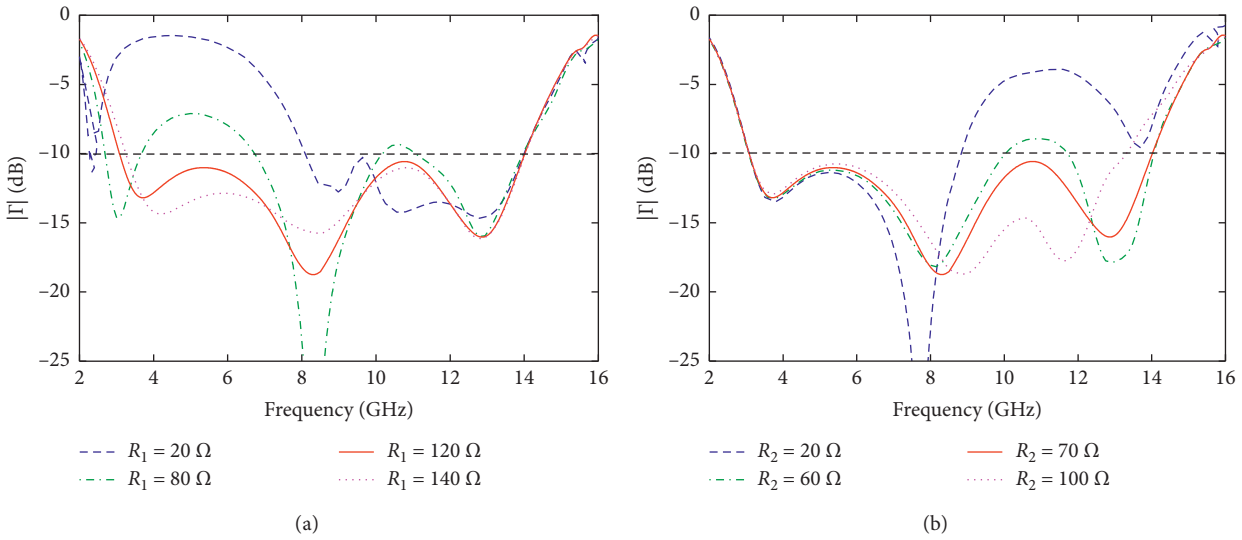


Figure 6: Different frequency responses of the proposed absorber with various values of chip resistors. (a) Different values of $R_1$. (b) Different values of $R_2$.

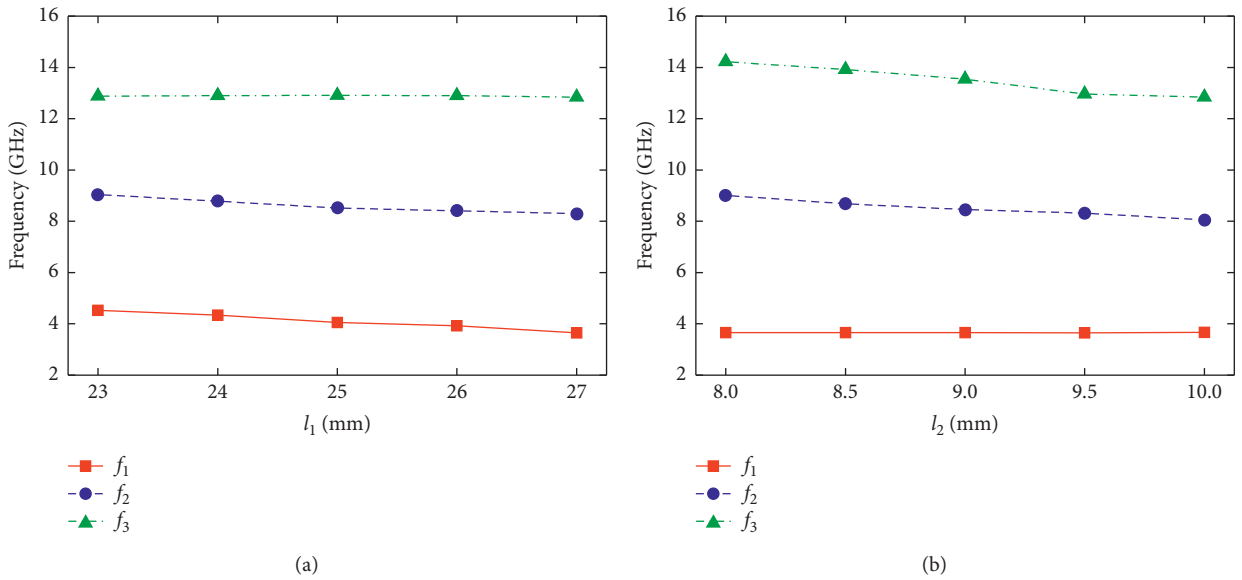


Figure 7: Variations of the reflection zero frequencies in the absorption band with respect to (a) the length $l_1$ of the longer strip and (b) the length $l_2$ of the shorter strip.

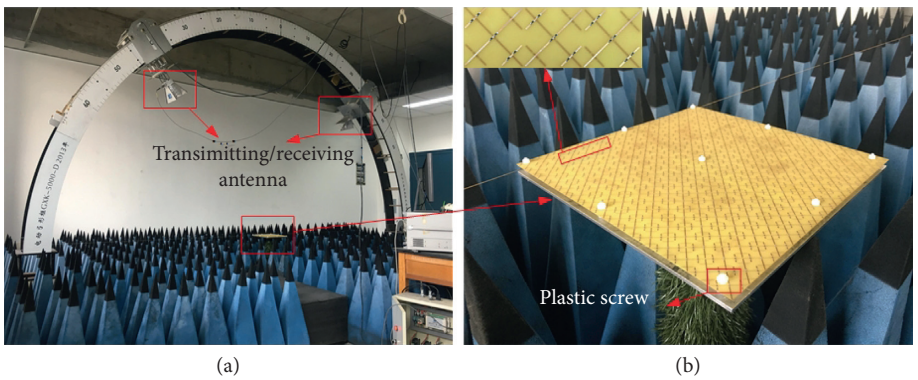


Figure 8: (a) Reflection measurement setup and (b) photograph of the prototype.

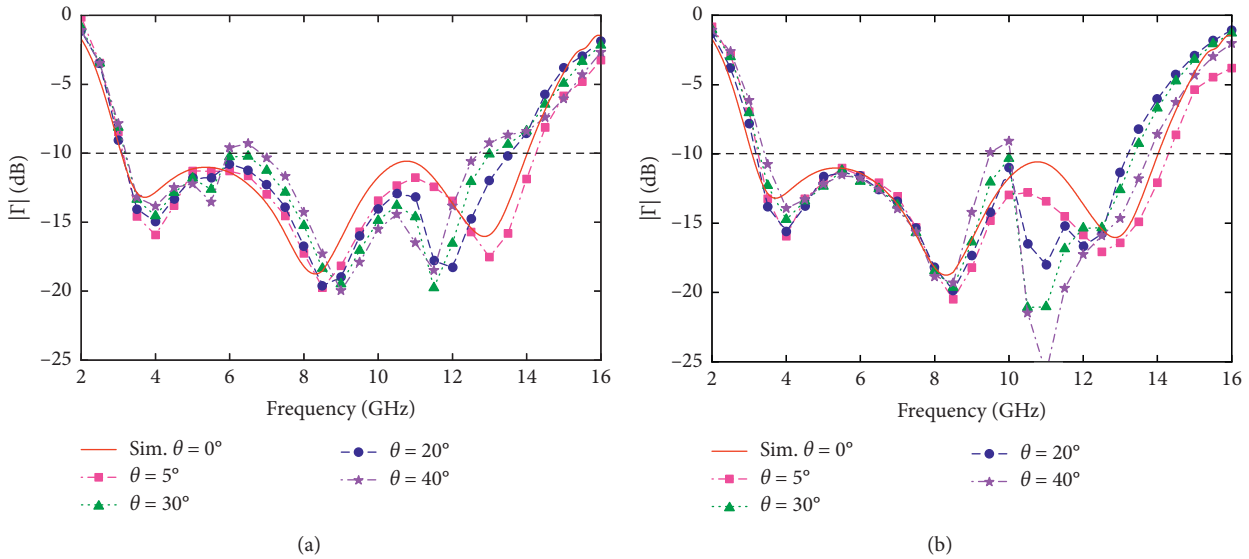


Figure 9: Simulated and measured results of the proposed absorber under oblique incidences for (a) TE polarization and (b) TM polarization.

Table 1: Performance comparison.

| Ref. | Thickness ($\lambda_{max}$) | FBW (%) | $(\lambda_{max} - \lambda_{min})/d$ | Oblique | Polarized |
|---|---|---|---|---|---|
| [1] | 0.077 | 70.7 | 6.67 | 30° | Dual |
| [10] | 0.071 | 92.2 | 8.85 | 30° | Dual |
| [11] | 0.08 | 127.9 | 9.7 | 30° | Dual |
| [12] | 0.088 | 126.8 | 8.63 | 30° | Dual |
| [17] | 0.1 | 112 | 7.17 | 30° | Single |
| [18] | 0.101 | 148 | 8.45 | 45° | Dual |
| [24] | 0.104 | 112 | 6.95 | 30° | Dual |
| [25] | 0.08 | 120 | 9.15 | 30° | Dual |
| This work | 0.08 | 129 | 9.46 | 30° | Dual |

The performance of our designed absorber is compared with the state-of-the-art absorbers in the literature, as shown in Table 1. It is shown that our proposed structure realizes an ultrawide absorption band for dual polarization, and its profile is only $0.08\lambda_L$. In addition, the ratio of wavelength difference to thickness in the operating band is utilized to intuitively evaluate the performance advantage, which can be expressed as the figure of merit $P$ [26]:

$$P = \frac{\lambda_{max} - \lambda_{min}}{d}, \tag{7}$$

where $\lambda_{min}$ and $\lambda_{max}$ are the minimum and maximum wavelengths in the operating band, respectively. Compared with other structures, our designed absorber has relatively better performance, considering bandwidth and thickness comprehensively.

## 4. Conclusion

This paper proposed a methodology for designing a low-profile wideband absorber, which has the stable angular and polarized responses. The proposed absorber is made up of a lossy layer with two orthogonal strips printed on both sides of a substrate and a metallic ground under the lossy layer. Arrays of two unequal metallic strips are printed on the substrate, and each strip is loaded with two resistors. By properly designing the resonant frequencies of these metallic strips, a wide absorption band with three resonances can be obtained. An example of the designed absorber is fabricated, and the measured results attest that it achieves an attractive wide absorption band for dual polarization and a stable angular response with a low-profile configuration.

## Data Availability

The data used to support the findings of this study are available from the corresponding author upon request.

## Conflicts of Interest

The authors declare that they have no conflicts of interest.

## Acknowledgments

This work was supported by the National Natural Science Foundation of China (NSFC) under Grant 61871036.

## References


[1] D. Kundu, A. Mohan, and A. Chakrabarty, "Single-layer wideband microwave absorber using array of crossed dipoles," *IEEE Antennas and Wireless Propagation Letters*, vol. 15, pp. 1589–1592, 2016.

[2] M. Olszewska-Placha, B. Salski, D. Janczak, P. R. Bajurko, W. Gwarek, and M. Jakubowska, "A broadband absorber with a resistive pattern made of ink with graphene nano-platelets," *IEEE Transactions on Antennas and Propagation*, vol. 63, no. 2, pp. 565–572, 2015.

[3] F. Costa, S. Genovesi, and A. Monorchio, "A chipless RFID based on multiresonant high-impedance surfaces," *IEEE Transactions on Microwave Theory and Techniques*, vol. 61, no. 1, pp. 146–153, 2013.

[4] R. L. Fante and M. T. McCormack, "Reflection properties of the salisbury screen," *IEEE Transactions on Antennas and Propagation*, vol. 36, no. 10, pp. 1443–1454, 1988.

[5] L. J. Du Toit, "The design of jauman absorbers," *IEEE Antennas and Propagation Magazine*, vol. 36, no. 6, pp. 17–25, 1994.

[6] K. N. Rozanov, "Ultimate thickness to bandwidth ratio of radar absorbers," *IEEE Transactions on Antennas and Propagation*, vol. 48, no. 8, pp. 1230–1234, 2000.

[7] B. A. Munk, *Frequency Selective Surfaces Theory and Design*, Wiley, Hoboken, NJ, USA, 2000.

[8] J. Lee and S. Lim, "Bandwidth-enhanced and polarisation-insensitive metamaterial absorber using double resonance," *Electronics Letters*, vol. 47, no. 1, pp. 8-9, 2011.

[9] Z. Shen, B. Zheng, Z. Mei, J. Yang, and W. Tang, "On the design of wide-band and thin absorbers using the multiple resonances concept," in *Proceedings of the 2008 International Conference on Microwave and Millimeter Wave Technology*, pp. 32–35, Nanjing, China, April 2008.

[10] M. Li, S. Xiao, Y. Bai, and B. Wang, "An ultrathin and broadband radar absorber using resistive FSS," *IEEE Antennas Wireless Propag. Lett*, vol. 11, pp. 748–751, 2012.

[11] B. Zhang, C. Jin, and Z. Shen, "Low-profile broadband absorber based on multimode resistor-embedded metallic strips," *IEEE Transactions on Microwave Theory and Techniques*, vol. 68, no. 3, pp. 835–843, 2020.

[12] Y. Shang, Z. Shen, and S. Xiao, "On the design of single-layer circuit analog absorber using double-square-loop array," *IEEE Transactions on Antennas and Propagation*, vol. 61, no. 12, pp. 6022–6029, 2013.

[13] Y. Han, W. Che, C. Christopoulos, Y. Xiong, and Y. Chang, "A fast and efficient design method for circuit analog absorbers consisting of resistive square-loop arrays," *IEEE Transactions on Electromagnetic Compatibility*, vol. 58, no. 3, pp. 747–757, 2016.

[14] S. Ghosh, K. V. Srivastava, and S. Bhattacharyya, "Design, characterisation and fabrication of a broadband polarisation-insensitive multi-layer circuit analogue absorber," *IET Microwaves, Antennas & Propagation*, vol. 10, no. 8, pp. 850–855, 2016.

[15] A. Kazemzadeh, "Thin wideband absorber with optimal thickness," in *Proceedings of the 2010 URSI International Symposium on Electromagnetic Theory*, pp. 676–679, Berlin, Germany, August 2010.

[16] A. K. Zadeh and A. Karlsson, "Capacitive circuit method for fast and efficient design of wideband radar absorbers," *IEEE Transactions on Antennas and Propagation*, vol. 57, no. 8, pp. 2307–2314, 2009.

[17] A. K. Rashid, Z. Shen, and S. Aditya, "Wideband microwave absorber based on a two-dimensional periodic array of microstrip lines," *IEEE Transactions on Antennas and Propagation*, vol. 58, no. 12, pp. 3913–3922, 2010.

[18] A. A. Omar and Z. Shen, "Double-sided parallel-strip line resonator for dual-polarized 3-D frequency-selective structure and absorber," *IEEE Transactions on Microwave Theory and Techniques*, vol. 65, no. 10, pp. 3744–3752, 2017.

[19] J. Mou and Z. Shen, "Design and experimental demonstration of non-Foster active absorber," *IEEE Transactions on Antennas and Propagation*, vol. 65, no. 2, pp. 696–704, 2017.

[20] J.-S. Hong and M. Lancaster, *Microstrip Filters for RF/Microwave Applications*, Wiley, Hoboken, NJ, USA, 2001.

[21] Q. Zhang, Z. Shen, J. Wang, and K. S. Lee, "Design of a switchable microwave absorber," *IEEE Antennas and Wireless Propagation Letters*, vol. 11, pp. 1158–1161, 2012.

[22] C. K. Lee and R. J. Langley, "Equivalent-circuit models for frequency-selective surfaces at oblique angles of incidence," *IEE Proceedings H Microwaves, Antennas and Propagation*, vol. 132, no. 6, pp. 395–399, 1985.

[23] R. J. Langley and E. A. Parker, "Equivalent circuit model for arrays of square loops," *Electronics Letters*, vol. 18, no. 7, pp. 294–296, 1982.

[24] F. Costa, A. Monorchio, and G. Manara, "Analysis and design of ultra thin electromagnetic absorbers comprising resistively loaded high impedance surfaces," *IEEE Transactions on Antennas and Propagation*, vol. 58, no. 5, pp. 1551–1558, 2010.

[25] S. Baghel, A. Mohan, and A. Chakrabarty, "Design and analysis of printed lossy capacitive surface based ultra-wideband low-profile absorber," *IEEE Transactions on Antennas and Propagation*, vol. 67, no. 5, pp. 3533–3538, 2019.

[26] K. N. Rozanov and S. N. Starostenko, "Numerical study of bandwidth of radar absorbers," *The European Physical Journal Applied Physics*, vol. 8, no. 2, pp. 147–151, 1999.